Journal of Applied Electrochemistry (2007) 37:71–76
DOI 10.1007/s10800-006-9217-9

Kinetics of the electrochemical oxidation of organic compounds at BDD anodes: modelling of surface reactions

MICHELE MASCIA*, ANNALISA VACCA, SIMONETTA PALMAS and ANNA MARIA POLCARO
Dipartimento di Ingegneria Chimica e Materiali, Università degli Studi di Cagliari, Piazza d'Armi, 09123, Cagliari, Italy
*(*author for correspondence, tel.: + 390706755059, fax: + 390706755067, e-mail: mmascia@dicm.unica.it)*

Received 14 February 2006; accepted in revised form 24 April 2006

Key words: BDD anodes, electrochemical oxidation, mathematical model, numerical prediction, organic compounds

Abstract

This paper presents the results of a numerical study of the kinetics of electrochemical oxidation of different organic substances at boron doped diamond (BDD). It is well established that oxidation of organics at BDD anodes takes place in the potential region of oxygen evolution, through reaction steps in which OH radicals are involved: these radicals can react with organic compounds to give more oxidised substances, or with water to give oxygen. Because of the high reactivity of OH radicals these reactions are confined to a thin film adjacent to the electrode surface. A mathematical model was implemented, which accounts for chemical and electrochemical reactions, as well as for the transport phenomena involved in the process: the parameters of the model were derived from experimental data. The model allowed calculation of the trend with time of reactant concentration, reaction intermediates and oxidisable agents: their space profiles in the reactor were also obtained. The numerical predictions of the model were compared with experimental results obtained from galvanostatic electrolyses of different organic compounds: (a) 2,4,6-trihydroxy-1,3,5 triazine also known as cyanuric acid (CA), which is well known to be refractory to oxidation with OH; (b) atrazine (ATR) the most oxidisable precursor of CA, and (c) phenol which is considered as an OH scavenger because of its high reactivity. The agreement between experimental and model predicted data was good in all the examined conditions.

List of symbols

a	Specific electrode area $a = \frac{A}{V}$ (m^{-1})
A	Electrode area (m^2)
C_i	Concentration of the ith compound (mol m^{-3})
d	Nozzle diameter (m)
D_i	Diffusivity of the ith compound (m^2 s^{-1})
F	Faraday number (C mol^{-1})
i	Current density (A m^{-2})
i_{lim}	Limiting current density (A m^{-2})
k_i	OH-organic specific reaction rate (dm^3 mol^{-1} s^{-1})
k_{m}	Mass transfer coefficient (m s^{-1})
k_{OH}	OH deactivation specific reaction rate (s^{-1})
Re	Reynolds number $Re = \frac{vd\rho}{\mu}$
Sc	Schmidt number $Sc = \frac{\mu}{\rho D_i}$
Sh	Sherwood number $Sh = \frac{k_{\mathrm{m}}d}{D_i}$
V	Volume of solution (m^3)

Greek symbols

δ	Diffusion layer thickness $\delta = \frac{D_i}{k_{\mathrm{m}}}$ (m)
μ	Viscosity of electrolyte (kg m^{-1} s^{-1})
ν	Linear velocity in the nozzle (m s^{-1})
ρ	Density of electrolyte (kg m^3)

1. Introduction

Good results in organic removal were obtained using boron doped diamond (BDD) electrodes at which it is generally assumed that oxidation takes place in the potential region of oxygen evolution through reaction steps in which OH radicals are involved [1–3]. These radicals react with organic compounds to give more oxidised substances, but they can also react with each other, with water or with inorganic compounds present in the solution to give oxygen or long-life oxidising agents. Because of the high reactivity of OH radicals, the volume in which the reactions occur is a thin film adjacent to the electrode surface. The OH-mediated mechanism allows complete combustion of organics at high reaction rates. Substances such as phenol are removed from aqueous solution through processes controlled by the mass transfer of the reactant from the bulk of the solution to the anodic surface [4]. High removal rates were also obtained for substances which are well known to be refractory to oxidation with OH, such as cyanuric acid (2,4,6-trihydroxy-1,3,5 triazine): however, in this case the reaction rate was affected both by mass transfer and current density at relatively high values of applied current densities [5].

In any case mass transfer plays an important role in the oxidation process and a suitable cell design is required to achieve the high removal rates allowed by the BDD anode. The reactor design also affects other variables that are crucial for the performance of the whole electrochemical plant, such as energy consumption and pressure drop.

Despite work on mathematical modelling and optimisation of cell configuration for the case of oxidation at active electrodes, only recently has the problem been examined for non active electrodes. Preliminary studies were devoted to the optimisation of parallel plate reactors [4, 6]; good performances were also obtained by using an impinging-jet configuration [5, 7, 8]. A model was developed to quantify the decrease in chemical oxygen demand (COD) during electrochemical oxidation of several substances in a parallel plate system [2, 4]. The process was described for two cases: in the first the process was controlled by the charge supplied and the oxidation rate described by zero-order kinetics; in the second case the reaction was controlled by mass transfer and an exponential decrease in COD with time was described by a first order law in which the specific reaction rate was the mass transfer coefficient.

The model proposed by Canizares et al. [9] represented the electrochemical reactor as a combination of three interconnected stirred-tank reactors: two of these reactors represented the cathodic and anodic reaction zones, with a volume represented by the diffusion layer, while the third reactor represented the mass transport zone. The diffusion layer was assumed as reaction zone for the oxidation of organics by oxidising radicals, and the kinetics of organic oxidations was described by pseudo-first order reactions.

In the present work, a different approach is followed: the electrochemical reactor is considered as a combination of reactors in which only the bulk is represented by a stirred-tank reactor. A diffusion-reaction model is used to model the diffusion layer: the reaction rates are described by second order kinetics with respect to organic and OH radicals concentrations. The model has been validated with respect to experimental results from electrochemical oxidation of different organic compounds. Because of the different behaviour they showed towards oxidation by OH radicals [5, 8], phenol, atrazine (ATR) and cyanuric acid (CA) were selected as model substances.

2. Mathematical model

Electrochemical oxidation of organic compounds at BDD anodes is not a direct conversion to CO_2 but occurs through the generation of reaction intermediates. Generation of aromatic and aliphatic compounds was observed during oxidation of phenol and phenolic compounds [7]; reaction pathways based on reaction in series were also observed during electrolyses of aqueous solution containing polyhydroxybenzenes [10], 4-nitrophenol [11], triazinic compounds [5], and dichloroaniline [8]. The apparent direct mineralization observed during electrochemical oxidation of phenol and other organic compounds under specific experimental conditions [4–6, 8] can be attributed to the high value of the ratio between the current density and the limiting current density for the mineralization of the reactant adopted. Under these experimental conditions, the flux of OH radicals is always higher than that required for the first oxidative steps. Thus, the excess OH radicals remain available for the further steps which lead to complete mineralization, and no reaction intermediates are detected in the bulk of the solution [7].

Based on the considerations reported above, the kinetic equation for the reaction of the generic ith compound with OH radicals ($C_i + \mathrm{OH} => C_{i+1}$) can be written as:

$$\frac{dC_i}{dt} = k_{i-1}C_{i-1}C_{\mathrm{OH}} - k_iC_iC_{\mathrm{OH}} \tag{1}$$

The different processes involved in the electrochemical removal of organic compounds from aqueous solutions are accounted for by the model: in the bulk of the solution (B) the mass balance of the ith compound can be represented by a mass transfer equation:

$$\frac{dC_i{}^{\mathrm{B}}}{dt} = ak_{\mathrm{m}}\left(C_i^{\mathrm{S}} - C_i{}^{\mathrm{B}}\right) \tag{2}$$

In the diffusion layer (DL) diffusion and reaction of organic compounds and OH radicals occur. The organic compounds are generated and consumed by chemical reactions mediated by OH radicals, and their mass balance can be represented by a diffusion-reaction equation:

$$\frac{dC_i{}^{\mathrm{DL}}}{dt} = D_i\frac{\partial^2 C_i{}^{\mathrm{DL}}}{\partial x^2} + k_{i-1}C_{i-1}{}^{\mathrm{DL}}C_{\mathrm{OH}} - k_iC_i{}^{\mathrm{DL}}C_{\mathrm{OH}} \tag{3}$$

where the terms on the right side represent diffusion, generation and consumption of the ith compound, respectively.

The reaction of OH radicals with water to give oxygen may occur through different pathways in which different transients of water are involved. In this work first order kinetics were adopted to describe these reactions, and a lumped kinetic constant k_{OH} was used.

The mass balance of the OH radicals is thus the following:

$$\frac{dC_{\mathrm{OH}}{}^{\mathrm{DL}}}{dt} = D_{\mathrm{OH}}\frac{\partial^2 C_{\mathrm{OH}}{}^{\mathrm{DL}}}{\partial x^2} - \sum_i k_iC_i{}^{\mathrm{DL}}C_{\mathrm{OH}} - k_{\mathrm{OH}}C_{\mathrm{OH}} \tag{4}$$

In Equation (4), the reactions of OH radicals with organic compounds are indicated, along with the deactivation of the radicals. This reaction is represented by first order kinetics in which the constant k_{OH} is a lumped parameter used to quantify the effect of the different deactivation reactions.

Equations (1–4) were numerically solved with the following initial conditions:

$$\begin{aligned} &C_{\mathrm{OH}}{}^{\mathrm{DL}} = 0 \\ &C_i{}^{\mathrm{DL}} = C_i{}^{\mathrm{B}} = C_{i0} \quad \forall x \end{aligned} \tag{5}$$

The boundary conditions for Equation (4) must be written by considering that the flux of OH radicals at the anode surface is a function of the current density through Faraday's law:

$$D_{\mathrm{OH}} \frac{\partial C_{\mathrm{OH}}}{\partial x} = -\frac{I}{AF} \quad x = 0 \tag{6}$$

The other boundary conditions are the following:

$$\begin{aligned} &D_i \frac{\partial C_i^{\mathrm{DL}}}{\partial x} = 0 \quad x = 0 \\ &C_i^{\mathrm{DL}} = C_i^{\mathrm{B}} \quad x = \delta \\ &C_{\mathrm{OH}} = 0 \quad x \Rightarrow \infty \end{aligned} \tag{7}$$

The model equations were numerically solved by finite element software: the numerical solution of the equations allows us to predict the trend in time of the different compounds in the bulk of solution, as well as the evolution of the space profile of the species considered.

3. Model validation

Phenol, CA and ATR were used as model compounds because of their different behaviour with respect to oxidation by OH radicals.

Electrochemical oxidation of phenol and phenolic compounds at BDD anodes has been extensively studied [12, 13]: the removal of phenol is a mass transfer controlled process, and the global reaction path is the following:

$$\text{Phenol} => \text{cyclic intermediates} => \text{aliphatic acids} => \mathrm{CO_2}$$

Distribution of intermediates only depends on the ratio between the current density and the limiting current density for the mineralization of the reactant [2, 8]: at high current density, low concentration and low mass transfer rate, phenol is directly converted to CO_2 and H_2O; at lower current density and higher phenol concentration, conversion to benzoquinone, hydroquinone and catechol may be observed, and in this case the concentration of phenol linearly decreases with the specific charge [6].

Cyanuric acid is known to be refractory to most OH based processes [14, 15], and the oxidation of CA by photochemical processes is effective only at high OH concentration [16, 17]. Electrochemical oxidation of CA at BDD anodes was found to be under kinetic control and strongly affected by the pH of the solution [5]. A high reaction rate, near to that corresponding to a mass transfer controlled process, was observed only at neutral pH and high current density. Reaction intermediates were not observed, and only inorganic nitrogen compounds were detected, in stoichiometric amounts, as final products of the reaction.

A different reaction path was observed for ATR oxidation [8]:

$$\text{ATR} => \text{CA} => \mathrm{CO_2} + \text{inorganic nitrogen compounds } (\mathrm{NO_3^-} \text{ and } \mathrm{NH_4^+}).$$

In this case, different concentrations of CA were always measured, although the ratio between current density and limiting current density for the mineralization of the reactant was high.

Experimental data obtained from galvanostatic electrolyses of Phenol, CA and ATR carried out with an impinging jet flow cell [7] were used to validate the numerical predictions of the model.

The values of the parameters used in the model equations are reported in Table 1, along with the corresponding sources. Mass transfer coefficients (k_{m}) used in the model were calculated by a dimensionless relation obtained in previous work [7]:

$$Sh = 0.02 Re^{0.8} Sc^{\frac{1}{3}} \tag{8}$$

The nozzle diameter (d = 3 mm) is assumed as characteristic length to calculate the dimensionless Sherwood, Schmidt and Reynolds numbers in Equation (8).

The diffusion coefficients of the organic compounds were evaluated by the correlation proposed by Wilke and Chang [18] and the diffusion coefficient for the self-diffusion of water was adopted for the OH radicals [19].

The kinetic constants for the reaction of OH radicals with phenol to give aromatic intermediates and with

Table 1. Values of the parameters adopted in the model

Kinetic constants/dm^3 mol^{-1} s^{-1}	Phenol	1.4×10^{10b}
	Aromatic intermediates	9×10^{8}
	Aliphatic acids	0.7×10^{8b}
	ATR	8×10^{9}
	CA (pH = 1)	0.6×10^{9}
	CA (pH = 1.8)	0.28×10^{8}
	CA (pH = 3)	0.44×10^{8}
	CA (pH = 7)	9×10^{9}
	CA (pH = 8)	2.1×10^{8}
	CA (pH = 12)	0.17×10^{8}
OH deactivation kinetic constant/s^{-1}		0.9×10^{10}
Diffusivity coefficients/m^2 s^{-1}	Organic compounds	9×10^{-10}
	OH radicals	2.3×10^{-10a}

[a] Kicuchi et al. 1997 [19].

[b] Ross and Ross 1977 [20].

aliphatic acids to give CO_2 were taken from the literature [20]. The constants related to the oxidation of aromatic compounds ATR and CA were adjustable parameters of the model. The values of these parameters were calculated through sensitivity analysis from the trend with time of the reactants, experimentally measured: each constant was obtained by a single set of experimental data.

The value of the parameter k_{OH} was obtained from data of phenol oxidation at high values of current density ($I = 50$ mA cm^{-2}) and low mass transfer rate ($k_m = 1 \times 10^{-5}$ m s^{-1}).

Figure 1(A) and (B) show the comparison between experimental and model predicted data for electrochemical oxidation of phenol under different experimental conditions.

Data in Figure 1(A) were obtained at low current density and high mass transfer rate, while those in Figure 1(B) were related to oxidation of phenol at high current density and low mass transfer rate: the behaviour of the system is correctly predicted by the model. The oxidation reactions are in parallel with respect to OH radicals and the amount of radicals available for the oxidation of each compound in the reaction layer depends on the values of the specific reaction rates. As can be seen from Table 1, the values of the kinetic constant for phenol and its oxidation intermediates are very different and in the order $k_{\mathrm{Phenol}} >> k_{\mathrm{aromatics}} >> k_{\mathrm{aliphatics}}$.

The space profile of OH radicals is also predicted by the model. It is worth observing that in all the experimental conditions modelled the profiles calculated show that OH radicals are present only in a thin layer near the electrode surface. Examples of the numerical prediction of OH radical profiles are depicted in Figure 2.

The profile of OH radicals depends on the imposed current density: an increase from 10 mA cm^{-2} to 50 mA cm^{-2} leads to an increase in OH concentration of an order of magnitude. It can also be observed that at high current density the profile rapidly reaches a pseudo-steady state. The thickness of the reaction layer predicted by the model is in agreement with the literature: a thickness of 100 Å is reported for reaction zones in which OH radicals generated by photocatalytic processes are involved [21].

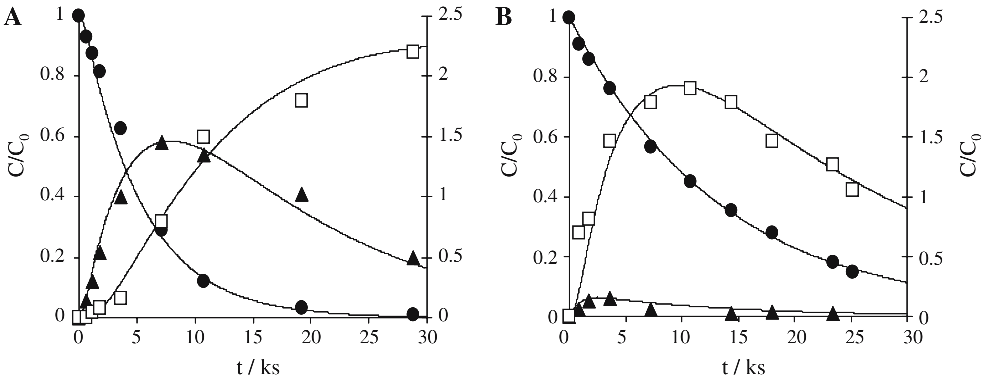

Fig. 1. (A) and (B) Comparison between experimental (symbols) and model predicted data for the trend in time of phenol (circles) aromatic intermediates (triangles) and aliphatic intermediates (empty symbols, secondary axis). Data from galvanostatic electrolyses of phenol in 0.1 M perchloric acid in different experimental conditions: $I = 1$ A and $k_m = 4 \times 10^{-5}$ m s^{-1} (A); $I = 0.3$ A and $k_m = 1.4 \times 10^{-4}$ m s^{-1} (B); values normalised with respect to the initial phenol concentration.

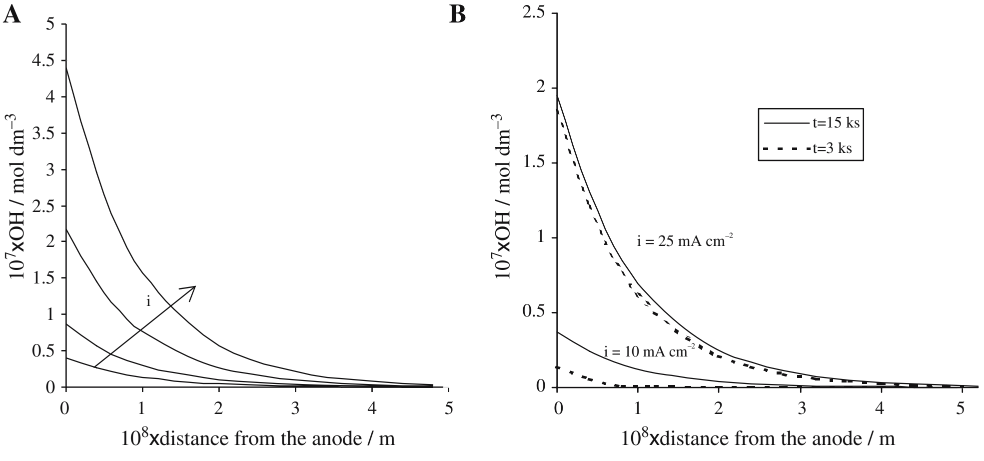

Fig. 2. (A) and (B) Space profiles of OH radicals concentrations calculated by the model. (A): 15 ks of electrolysis at different current densities; (B): 3 ks (dotted lines) and 15 ks (full lines) of electrolysis at different current densities.

The model predictions for electrochemical removal of (CA) at BDD anodes are reported in Figure 3 and are compared with the relevant experimental data. The proposed model allows quantitative interpretation of the strong effect of the solution pH on the process, experimentally evinced in terms of kinetic constant values: the curves in Figure 3 were obtained using the values of k_{CA} reported in Table 1.

The experimental data and the curves calculated by the model for ATR oxidation at BDD anodes are depicted in Figure 4, and in this case also the solid lines calculated by the model show good agreement with the experimental values: the trend in time of NO_3^- ions, which were detected as final products of ATR degradation, is also well interpreted.

4. Conclusions

A physically consistent mathematical model was developed to numerically predict the electrochemical oxidation of organics at BDD anodes. The proposed model accounts for the different phenomena involved in the process, such as diffusion and reaction near the electrode surface and OH radical generation at the anode surface. The model was used to interpret experimental data deriving from electrolyses of several organic compounds, characterised by different reactivity with OH radicals. Good agreement was obtained between calculated values and experimental data in a wide range of experimental conditions, indicating that the proposed model is a good representation of the physical system. Through the approach adopted in this work it was possible to separately quantify the effects of the main parameters of the process, the hydrodynamics of the cell, current density and the chemistry of system. The effect of chemical parameters can be effectively quantified by the values of the kinetic constants, which can be easily obtained from experimental data or from the literature. The proposed model can also be used to give information about the OH radical profiles in the reaction zone. The extent of this zone was calculated and the value obtained is in agreement with the literature.

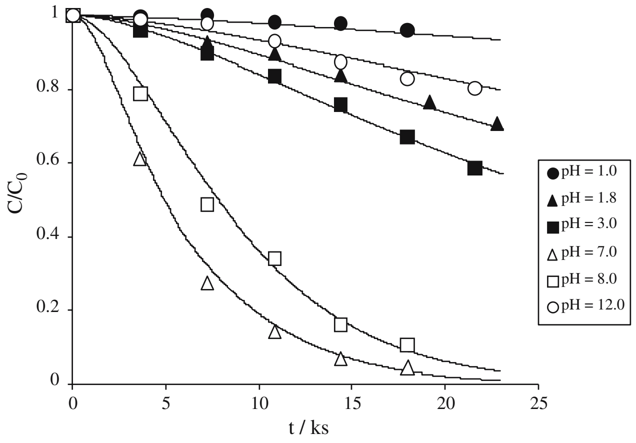

Fig. 3. Comparison between experimental (symbols) and model predicted data for electrochemical oxidation of CA at BDD anode at different pH values: $I = 300$ mA; $k_m = 4 \times 10^{-5}$ m s^{-1}; Values normalised with respect to the initial CA concentration.

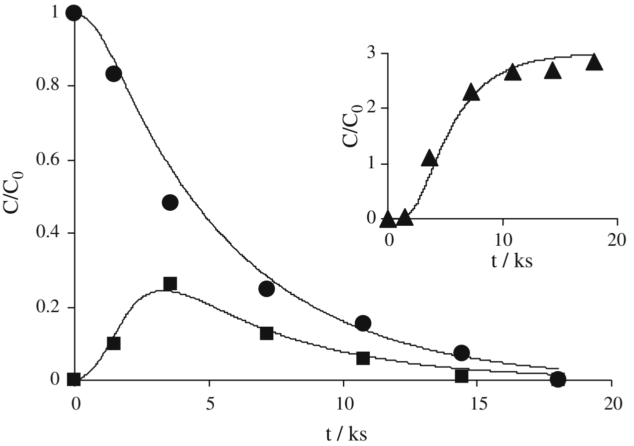

Fig. 4. Comparison between experimental (symbols) and model predicted data for the trend in time of ATR and CA concentration during electrochemical oxidation of ATR solutions at BDD anodes: inset shows the trend in time of NO_3^- ions concentration. $I = 0.3$ A; $k_m = 4 \times 10^{-5}$m s^{-1}; pH = 7; Values normalised with respect to the initial ATR concentration.

References

1. O. Simond, V. Schaller and C. Comninellis, *Electrochim. Acta* **13–14** (1997) 2009.
2. M. Panizza, P. Michaud, G. Cerisola and C. Comninellis, *Electrochem. Comm.* **3** (2001) 336.
3. L. Gherardini, P. Michaud, M. Panizza, G. Cerisola and C. Comninellis, *J. Electrochem Soc.* **D78** (2001) 148.
4. J. Iniesta, P. Michaud, M. Panizza, G. Cerisola, A. Aldaz and C. Comninellis, *Electrochim. Acta* **46** (2001) 3573.
5. A.M. Polcaro, M. Mascia, S. Palmas and A. Vacca, *Electrochim. Acta* **50** (2005) 1841.
6. M.A. Rodrigo, P. Michaud, I. Duo, M. Panizza, G. Cerisola and C. Comninellis, *J. Electrochem. Soc.* **148** (2001) D60.
7. A.M. Polcaro, M. Mascia, S. Palmas and A. Vacca, *J. Appl. Electrochem.* **33** (2003) 885.
8. A.M. Polcaro, M. Mascia, S. Palmas and A. Vacca, *Electrochim. Acta* **49** (2004) 649.
9. P. Canizares, J. Garcia-Gomez, J. Lobato and M.A. Rodrigo, *Ind. Eng. Chem. Res.* **43** (2004) 1915.
10. P. Cañizares, C. Sáez, J. Lobato and M.A. Rodrigo, *Ind. Eng. Chem. Res.* **43** (2004) 6629.
11. P. Cañizares, C. Sáez, J. Lobato and M.A. Rodrigo, *Ind. Eng. Chem. Res.* **43** (2004) 1944.
12. P. Cañizares, J. Lobato, R. Paz, M.A. Rodrigo and C. Sáez, *Wat. Res.* **39** (2005) 2687.
13. B. Nasr, G. Abdellatif, P. Cañizares, C. Sáez, J. Lobato and M.A. Rodrigo, *Environ. Sci. Technol.* **39** (2005) 7234.
14. E. Pelizzetti, V. Maurino, C. Minero, V. Carlin, M.L. Tosato, E. Pramauro and O. Zerbinati, *Environ. Sci. Technol.* **24** (1990) 1559.
15. A. Bozzi, M. Dhananjeyan, I. Guasaquillo, S. Parra, C. Pulgarin, C. Weins and J. Kiwi, *J. Photochem. Photobiol. A: Chem.* **162** (2004) 179.
16. C. Minero, E. Pelizzetti, S. Malato and J. Blanco, *Solar Energy* **56** (1996) 411.

17. Oh Young-Chul and W.S. Jenks, *J. Photochem. Photobiol. A: Chem.* **162** (2004) 323.
18. R.H. Perry and D.W. Green, *Perry's Chemical Engineers' Handbook*, 7th ed., (Mc Graw Hill, New York, 1997).
19. Y. Kicuchi, K. Sunada, T. Iyoda, K. Hashimoto and A. Fujishima, *J. Photochem. Photobiol. A: Chem.* **106** (1997) 51.
20. F. Ross and A.B. Ross, *Selected Specific Rates of Reactions of Transient from Water in Aqueous Solution III Hydroxyl Radical and Perhydroxyl Radical and their Radical Ions* (US Dept. of Commerce, Washington, 1977).
21. R. Hoffmann, S.T. Martin, W. Choi and D. Bahnemann, *Chem. Rev.* **95** (1995) 69.